doi: 10.34248/bsengineering.1664037



Research Article Volume 8 - Issue 5: 1440-1449 / September 2025

# UNVEILING ANTIBODY-MEDIATED ALLOSTERY IN INTERLEUKIN-1ß VIA CONFORMATIONAL SAMPLING AND **MACHINE LEARNING**

## Arzu UYAR1\*

İzmir Institute of Technology, Faculty of Engineering, Department of Bioengineering, 35433, İzmir, Türkiye

Abstract: Human interleukin-1 $\beta$  (IL-1 $\beta$ ), a pivotal proinflammatory cytokine, is a therapeutic target in autoimmune and inflammatory diseases. While antibodies blocking IL-1β signaling are effective, their allosteric mechanisms remain poorly understood. This study investigates how four distinct antibodies induce long-range allosteric effects in IL-1β, leveraging computational approaches to map allosteric communication and identify critical sites. Ensembles of apo and antibody-bound IL-1β states were generated using the enhanced conformational sampling technique ClustENMD, followed by the application of two different dimensionality reduction methods in machine learning (principal component analysis, PCA; linear discriminant analysis, LDA) to the generated conformers. PCA highlighted how diverse ensembles ClustENMD generated, while LDA revealed antibody-specific allosteric effects on the human IL-1β. By integrating conformational dynamics with machine learning, this work advances a predictive framework for engineering antibodies with tailored allosteric properties. The discovery of binding sites on IL-1 $\beta$  might further open avenues for drug design.

Keywords: Antibody, Allostery, Conformational sampling, ClustENMD, Machine learning

\*Corresponding author: İzmir Institute of Technology, Faculty of Engineering, Department of Bioengineering, 35433, İzmir, Türkiye E mail: arzuuyar@iyte.edu.tr (A. UYAR)

Arzu UYAR



https://orcid.org/0000-0003-2357-1941

Received: March 24, 2025 Accepted: July 23, 2025 Published: September 15, 2025

Cite as: Uyar A. 2025. Unveiling antibody-mediated allostery in Interleukin-1  $\beta$  via conformational sampling and machine learning. BSJ Eng Sci, 8(5): 1440-1449.

## 1. Introduction

The human interleukin-1  $\beta$  (IL-1 $\beta$ ) is a potent proinflammatory cytokine that plays a critical role in immune response. Changes in IL-1β regulation have been linked to many diseases, such as autoinflammatory diseases, type II mellitus, cardiovascular events, amyotrophic lateral sclerosis, as well as cancer (Dinarello, 2014; Guo et al., 2016; Ridker et al., 2017a; Ridker et al., 2017b; Wong et al., 2020; Diwanji et al., 2023). Therefore, IL-1 $\beta$  is one of the targets in the drug discovery field.

IL-1 $\beta$  is a monomeric protein with 269 residues (~31 kDa). It becomes active after the caspase-1 cleaves the structure. The resulting structure is the mature form of the IL-1 $\beta$  and contains 154 amino acids (~17 kDa). The mature form consists of 12 antiparallel beta-strands forming a  $\beta$ -barrel. Some of the loops connecting the  $\beta$ strands in the IL-1ß structure are responsible for the IL- $1\beta$  receptor (IL- $1\beta$ R) binding, and they form sites A and B as shown in Figure 1. Therefore, both sites are a focus of IL-1\beta drug discovery studies, and currently, 26 smallmolecules have been discovered targeting those sites in IL-1 $\beta$  (Berman et al., 2000).

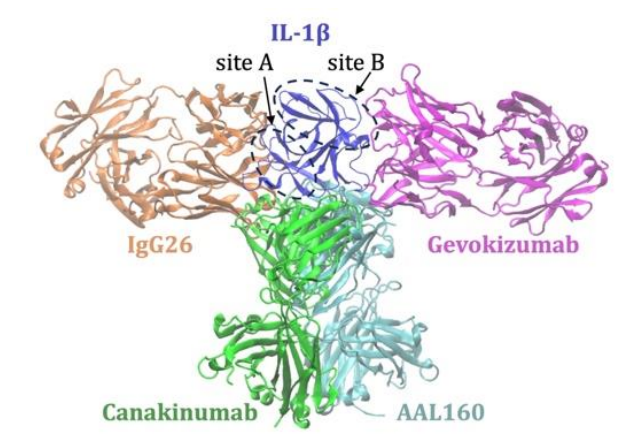


Figure 1. 3D structures of the IL-1β:IgG26 (orange), IL-1β:AAL160 (cyan), IL-1β:Canakinumab (green), and IL- $1\beta$ :Gevokizumab (magenta). Only the IL- $1\beta$  (dark blue) in the Gevokizumab-bound complex is shown for clarity. The figure is prepared using VMD (Humphrey et al., 1996).

In addition to small molecules, another way to regulate a protein structure is to develop antibodies that specifically bind to the target of interest. Antibodies are Y-shaped proteins and are increasingly preferred in the pharmaceutical sector due to their properties, such as

BSJ Eng Sci / Arzu UYAR 1440



high specificity and affinity for their targets and reduced side effects. Currently, five different fragment antigenbinding (Fab) structures have been specifically developed to target IL-1 $\beta$ . Four of them, namely IgG26, AAL160, Canakinumab, and Gevokizumab, have a full 3D structure. On the other hand, the fifth antibody, IgG26A, has missing residues and is an IgG26-derivative (Kuo et al., 2021).

IgG26 binds to the IL-1β epitope (site A) and simultaneously inhibits IL-1\beta R and IL-1\beta R accessory protein (IL-1RAcP) binding (PDB ID: 7chy) (Kuo et al., 2021). Also, AAL160 and Canakinumab interact with the IL-1 $\beta$  from a site with a slight overlap with the IgG26binding site; however, their binding poses are different than that of IgG26. AAL160 acts on a site in IL-1β different than the IL-1BR recognition site and interacts with some of the residues in site A (PDB ID: 7z4t) (Fischman et al., 2023). Similarly, the Canakinumab-bound crystal structure (PDB ID: 4g6j) indicates that the heavy-chain of the antibody binds to IL-1 $\beta$  from site A (Blech et al., 2013). On the other hand, Gevokizumab (PDB ID: 4g6m) binds to IL-1β from site B (Blech et al., 2013). It is claimed to be a regulatory therapeutic antibody that modulates IL-1β bioactivity by reducing the affinity for its IL-1\(\beta\rm{RI:IL-}\) 1βRAcP signaling complex (Owyang et al., 2011).

Interactions at the antibody:IL-1\beta interfaces were identified and explained in detail in the articles related to corresponding crystal structures (Blech et al., 2013; Owyang et al., 2011; Kuo et al., 2021; Fischman et al., 2023). However, elucidating long-range allosteric effects on IL-1β upon antibody binding was so far not available. Here, in this computational study, a comparison between four different antibody-bound IL-1β complexes and apo  $IL-1\beta$  was performed in atomistic detail using conformational sampling and machine learning. Several conformers for the bound complexes and apo IL-1 $\beta$  were generated using ClustENMD (Kaynak et al., 2021), a conformational sampling method. Then, these conformers were subjected to two different machine learning methods, Principal Component Analysis (PCA) and Linear Discriminant Analysis (LDA), to analyze the diversity of ensembles and detect any differences between antibodybound and apo IL-1β conformers.

# 2. Materials and Methods

# 2.1. Human IL-1ß Crystal Structures

Figure 1 shows the crystal structures of human IL-1 $\beta$  used in this study. Only one IL-1 $\beta$  structure (Gevokizumabbound form, 4g6m) is shown for clarity because there is no big structural difference in the antigen part of four different antibody-bound human IL-1 $\beta$ . In Figure 1, each antibody is colored differently, and well-known binding sites A and B are shown with dashed circles. The resolution values of each structure are as follows: Gevokizumab-bound (4g6m): 1.81 Å; Canakinumab (4g6j): 2.03 Å; IgG26 (7chy): 2.65 Å; AAL160 (7z4t): 3.30 Å. None of the structures has a mutation.

## 2.2. ClustENMD: Unbiased Conformational Sampling

The ClustENMD (Kaynak et al., 2021) provides an unbiased sampling of biomolecular structures such as proteins, protein-protein, and protein-nucleic acid complexes. It is a hybrid method that combines the Anisotropic Network Model (ANM) (Doruker et al., 2000; Atilgan et al., 2001), an Elastic Network Model, with molecular dynamics (MD) simulation. In ClustENMD, the initial structure is deformed along the linear combination of the slowest (softest) modes obtained from ANM, and several different conformers are generated. Then, the structural similarity values between these conformers are calculated using the root-mean-square deviation (RMSD) value, and this metric is used in hierarchical clustering of all conformers. Each cluster is represented by a cluster member. A short energy minimization is applied to each cluster member using OpenMM, an open-source MD program (Eastman et al., 2017; Eastman and Pande, 2010). The energetically minimized cluster members are subjected to the same process applied to the initial conformation, and thus, new generations (gens) are produced. Eventually, an ensemble of conformers is obtained for one ClustENMD run. In this study, a ClustENMD run is performed for each antibody-bound and apo IL-1β. The five slowest modes are used in ANM to generate nearly 2000 conformers from 10 generations in ClustENMD runs. Thus, all conformers are used in PCA and LDA analyses. The total number of conformers is higher than the number of features used in PCA and LDA analyses (see next section for details),

# 2.3. Principal Component Analysis (PCA)

Principal component analysis (PCA) (Amadei et al., 1993) is applied separately to the apo and antibody-bound IL-1 $\beta$  ensembles to extract essential modes (principal components, PCs). Only C $\alpha$  coordinates of all residues in the apo and antibody-bound IL-1 $\beta$  ensembles were extracted and used in PCA calculations. Each conformer is considered when calculating the covariance matrix in PCA. Eigenvector sets representing the first and second PCs are obtained for both apo and antibody-bound forms and used in projection calculations.

# 2.4. Linear Discriminant Analysis (LDA)

Linear Discriminant Analysis (LDA) is a supervised machine learning technique used for dimensionality reduction within multiclass data and class prediction of a new data point. LDA constructs a set of projection variables that aim to minimize the intra-class variance while simultaneously maximizing the inter-class separation.

In the context of protein dynamics, LDA serves as a valuable tool for discerning differences between various datasets and predicting the class index of novel conformations (Sakuraba and Kono, 2016; Uyar et al., 2018; Uyar and Dickson, 2021). In this study, two specific classes of IL-1 $\beta$  conformations, named "apo" and "complex", are used in LDA training and testing. Here, the features are the x, y, and z coordinates of all C $\alpha$  atoms in the apo and complex classes. LDA is applied to the data

sets using the Scikit-learn library (Pedregosa et al., 2011). The generated LDA models provide an LDA vector that separates two classes. The component of the LDA vector provides high fluctuating residues and, therefore, highlights the significant differences between classes.

## 3. Results

## 3.1. ClustENMD Conformers

Ensembles of unbiased ClustENMD conformers for the apo (Ab-removed) and antibody-bound IL-1 $\beta$  were shown in Figure 2. Here, IgG26 was colored in orange, whereas ALL160 was in cyan, Canakinumab in green, Gevokizumab in magenta, and the apo IL-1 $\beta$  in blue. Every  $50^{\rm th}$  conformer (gray cartoons) for each studied system was shown for clarity from the front and side views.

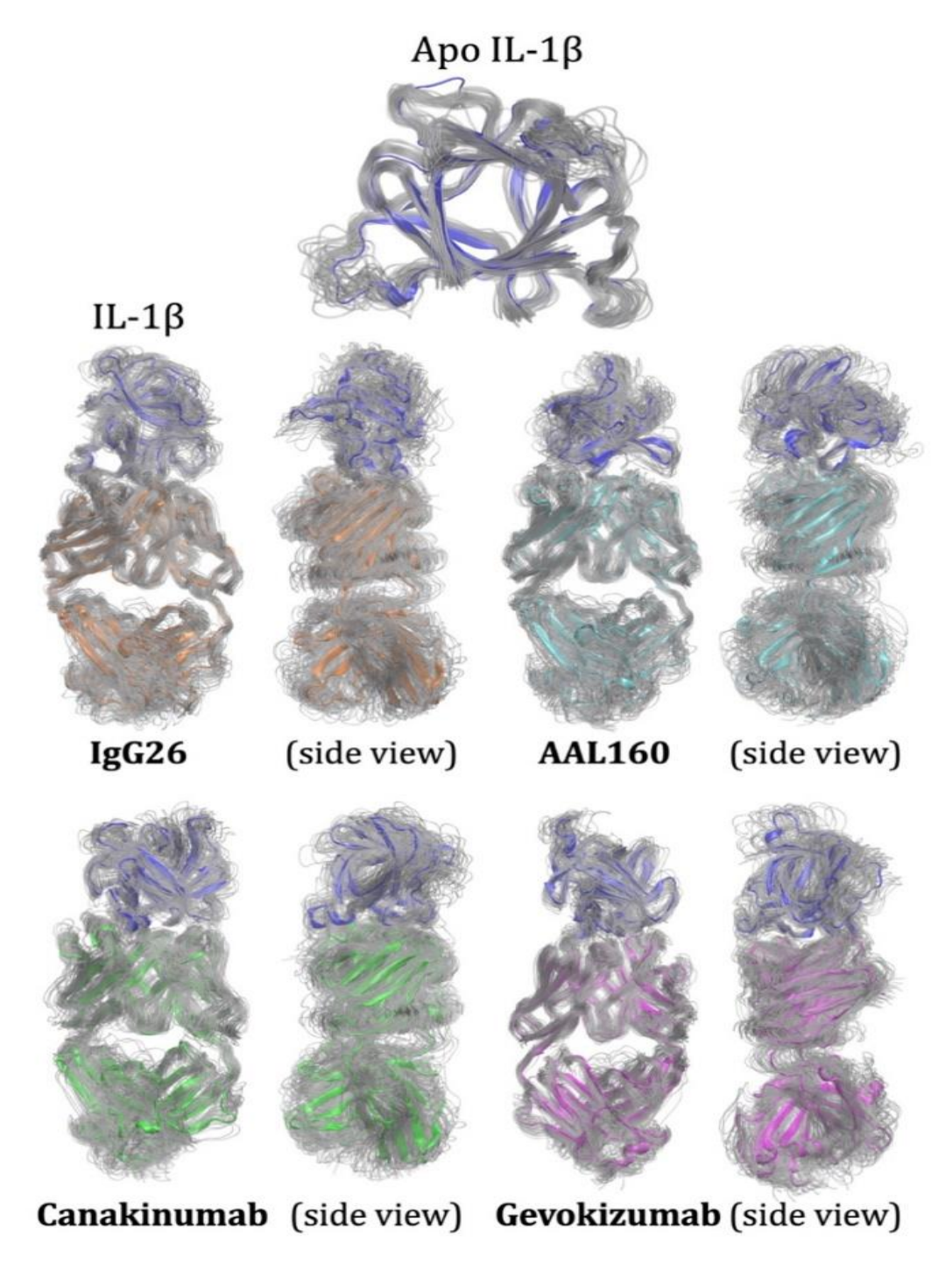


**Figure 2.** ClustENMD ensembles for the apo IL-1 $\beta$  (dark blue), IL-1 $\beta$ :IgG26 (orange), IL-1 $\beta$ :AAL160 (cyan), IL-1 $\beta$ :Canakinumab (green), and IL-1 $\beta$ :Gevokizumab (magenta). Every 50<sup>th</sup> conformer is shown for each structure for clarity. The figure is prepared using VMD (Humphrey et al., 1996).

RMSD values with respect to the initial conformer were calculated for each conformer (without skipping any frame), and their median and maximum RMSD values were given in Table 1 for each studied system. The

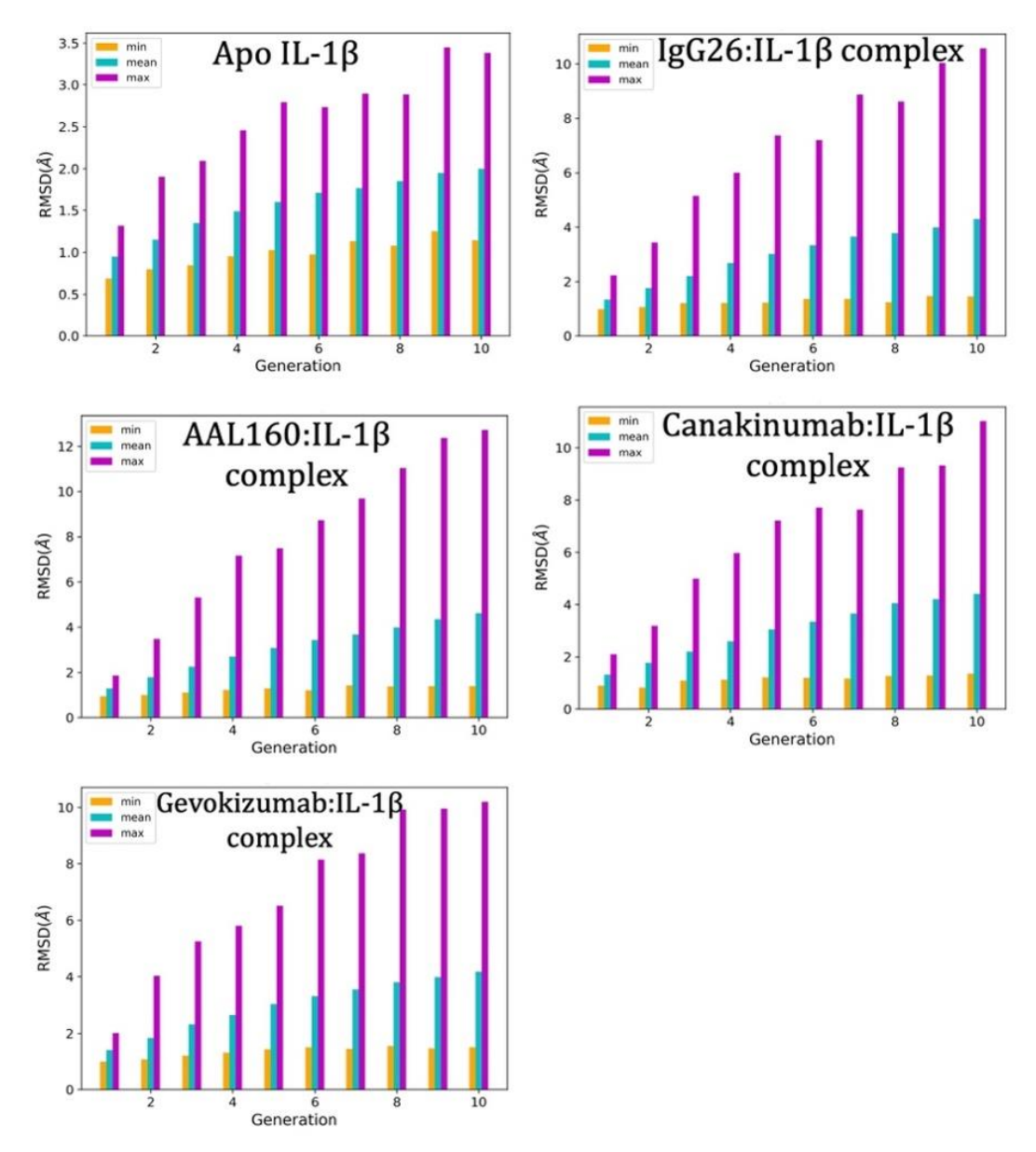
conformers generated for the apo IL-1 $\beta$  reached near 3.5 Å. Antibody-bound forms were more flexible and produced higher RMSD values between 10.2-12.7 Å.

Table 1. The median and maximum RMSDs with respect to the initial conformer for each studied system for IL-1β.

System (PDB ID)	Median RMSD (Å)	Max RMSD (Å)
Ab-removed IL-1β (4g6m)	1.66	3.45
IgG26:IL-1β (7chy)	2.85	10.57
AAL160:IL-1β (7z4t)	2.97	12.71
Canakinumab:IL-1β (4g6j)	2.94	11.02
Gevokizumab:IL-1β (4g6m)	2.97	10.20

A similar RMSD calculation was done for each generation and is given in Figure 3. Here, the figure shows the minimum (min), mean, and maximum (max) RMSD of the conformers in each generation with respect to the initial conformation where the min is in orange, the mean in

cyan, and the max in magenta. As expected, it can be seen that the RMSD values increased when the number of generations used in the ClustENMD calculation was increased.



**Figure 3.** The min, mean, and max RMSD of the conformers in each generation with respect to the initial conformation of IL-1β.

#### 3.2. PCA Analysis

Progression of the apo conformers in generations is shown by projecting them onto PC1 and PC2 (top panel in Figure 4). Here, the initial conformation of the apo IL-1 $\beta$  is highlighted with a red star, whereas the apo conformers coming from 10 different generations are colored differently. It was observed that most conformers were grouped in similar regions; however, gen 5 and later generations produced distinct conformers, which sampled different spots in the conformational space.

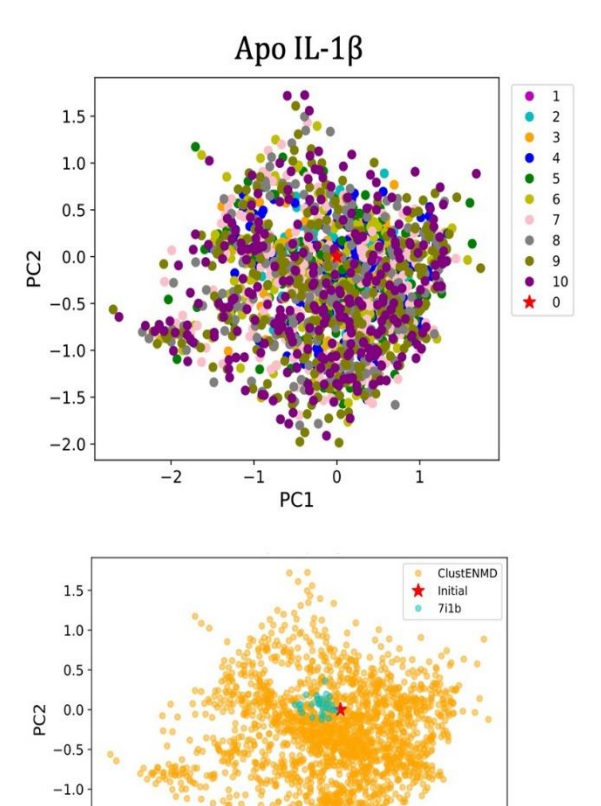


**Figure 4.** Projection of IL-1 $\beta$  conformers onto the PC1 and PC2. In the top panel, a projection of apo IL-1 $\beta$  conformers obtained from 10 generations is given. The red star represents the initial structure. Each generation is shown in different colors. A projection of the NMR structure of IL-1 $\beta$  (PDB ID: 7i1b) having 32 conformers (cyan) is also given in the bottom panel.

An NMR structure for IL-1 $\beta$  is available and has 32 conformers. These NMR conformers were also projected onto the same two principal components to see if the unbiased ClustENMD conformers yield structures similar to those of the NMR ensemble (bottom panel in Figure 4). Here, the unbiased ClustENMD conformers for the apo structure are in orange, and NMR conformers are in cyan dots. It was observed that ClustENMD produced conformers similar to the NMR conformers in addition to distinct conformers that are pretty different than the NMR conformers.

PCA analysis was also performed for each antibody-bound IL-1 $\beta$  structure. Here, the initial conformation of each antibody-bound IL-1 $\beta$  is highlighted with a red star, whereas the conformers in different generations are colored differently. Again, it was observed that most of the conformers were near the initial complex structure; however, generations after gen 5 produced distinct antibody-bound conformers for IL-1 $\beta$  that were in the different regions of the conformational space.

PCA is an unsupervised machine learning method and is suitable for maximizing the variance in data. However, PCA is not very effective in comparing two distinct classes, such as apo and antibody-bound ensembles. Therefore, next, another machine learning method, Linear Discriminant Analysis (LDA), was applied to ClustENMD conformers.

#### 3.3. LDA Analysis

All conformers from the apo and IL-1ß part of each antibody-bound IL-1ß ensemble were merged into two sets, apo and bound. Thus, four different apo-bound set pairs were obtained. LDA was separately applied to all pairs to detect significant differences in each set. The yielded first LDA mode vectors that separate the two data sets were used for projection. The densities of the projection values were calculated and given in Figure 6, where the apo IL-1 $\beta$  is in blue and antibody-bound in orange. All apo and complex conformers were well separated using the corresponding first LDA mode vector, except Gevokizumab-bound IL-1\beta, where slight overlap was observed between the apo and complex conformers. Next, the first LDA mode vectors obtained from each LDA analysis were used to calculate residue displacements in IL-1 $\beta$  for each structure. Figure 7 shows the residue fluctuations of IL-1 $\beta$  in each antibody-bound complex. Here, in each panel, the IL-1\beta structure is colored according to the residue fluctuation values obtained from the corresponding LDA mode vector using a rainbow color code. The high fluctuating residues are represented by red and orange, and the lowest fluctuating residues are in dark blue. The corresponding antibody binding sites are also marked with dashed dark gray circles in Figure 7. The IL-1ß residue fluctuations in the first LDA mode vectors showed that the LDA analysis for the IgG26- and Canakinumab-bound IL-1\beta structures revealed very dominant single residues (one for each structure). K109 near site B is the only key residue revealed from the LDA analysis for the IgG26-bound (7chy) structure (top left in Figure 7). Clearly, the dominance of K109 in LDA fluctuations suppresses the other residues. In fact, eight more residues, N129 and P131 in the binding site A; L110 in site B; as well as S17, Y24, E111, F112, and V132 contribute to the conformational differences between the apo and antibody-bound IL-1β when the high fluctuating K109 is omitted in the calculation (top center in Figure 7). In the case of Canakinumab, L67 appears as the only key residue (bottom left in Figure 7). Similar to the IgG26, single residue dominance is present in the LDA mode.

-1.5

-2.0

When the dominant L67 is omitted, it is observed that K65, N66, K109 (near site B), and D145 also contribute to the conformational difference in IL-1 $\beta$  conformers (bottom center in Figure 7). Here, only K65 is an antibody-

interacting residue, which makes both H-bond and non-bonded interactions with the heavy chain of Canakinumab.

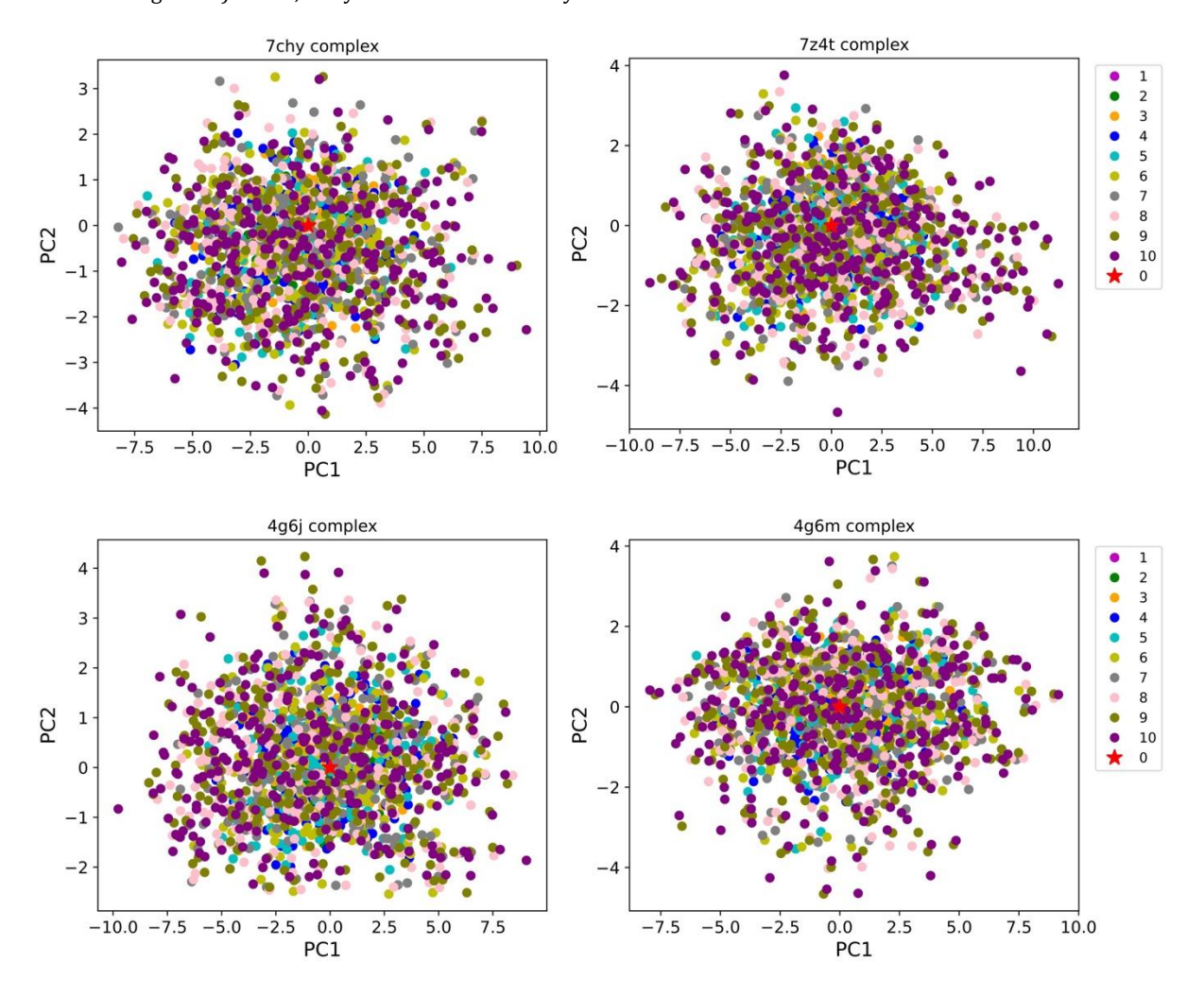


**Figure 5.** Projection of the antibody-bound (complex) IL-1 $\beta$  conformers: IgG26: 7chy, AAL160: 7z4t, Canakinumab: 4g6j, and Gevokizumab: 4g6m. Conformers in different generations are colored differently, as shown in the color legend. The red star represents the initial structure.

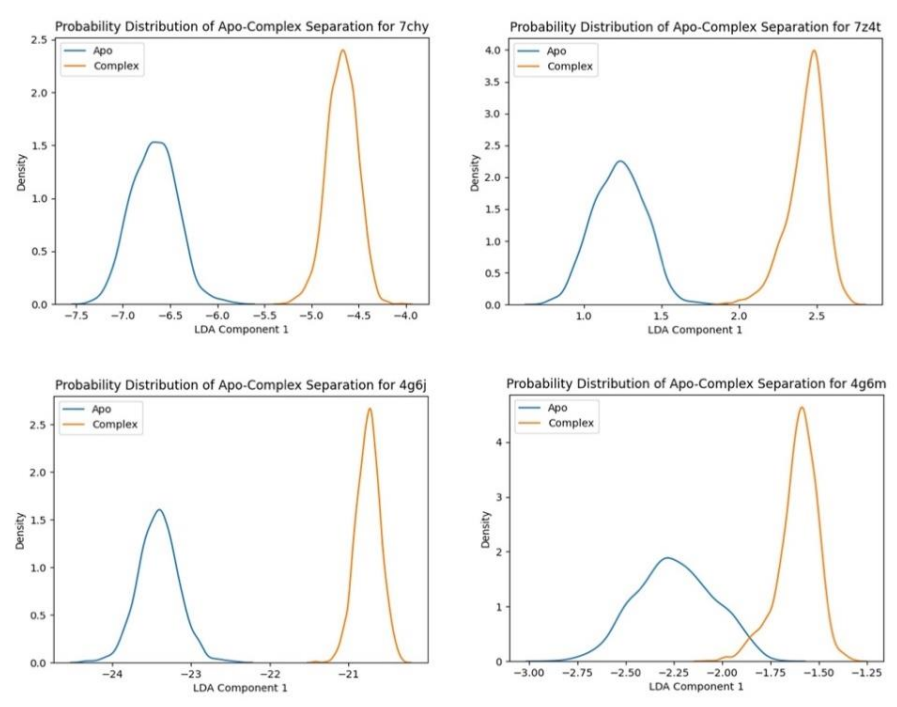


**Figure 6.** Distributions of the LDA projections of four antibody-bound IL-1β conformers. IgG26: 7chy, AAL160: 7z4t, Canakinumab: 4g6j, and Gevokizumab: 4g6m.

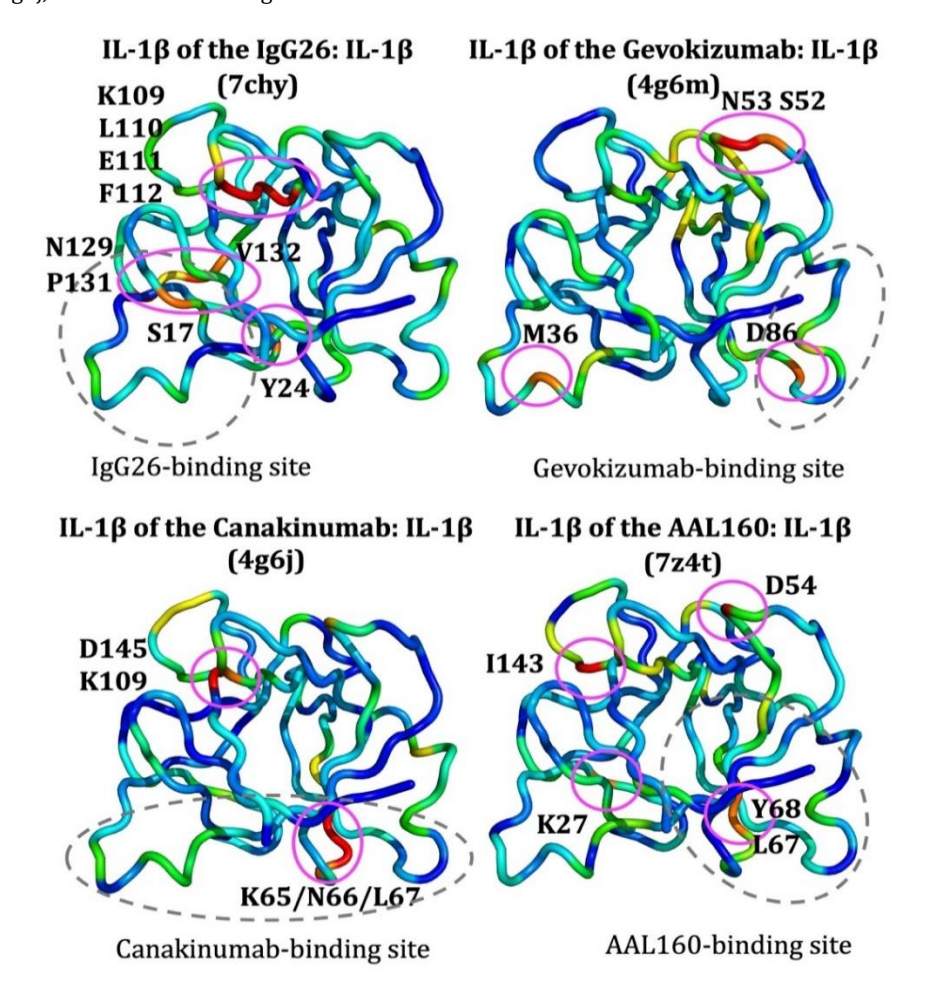


**Figure 7.** Residue fluctuations in the first LDA mode vectors for the corresponding structures. The structures are colored individually according to the residue fluctuation values using a rainbow color code. Red represents the highest fluctuating residues, whereas dark blue represents the lowest fluctuating residues. High fluctuating residues (red and orange) are marked with magenta circles, and their one-letter codes are written on each structure. The corresponding antibody binding sites are marked with dashed dark gray circles. The figure is prepared using PyMOL (DeLano, 2020).

On the other hand, Gevokizumab and AAL160 antibodies revealed more key residues in their first LDA mode, showing conformational differences in IL-1 $\beta$  conformers. In the Gevokizumab-bound IL-1 $\beta$  (top right in Figure 7), the most critical residue is N53, which is far from the antibody binding site; however, this residue is one of the residues in site B. Its neighbor S52 was also revealed as important. In addition, Gevokizumab-bound conformers yielded two more key residues: D86 in the Gevokizumab-binding site and M36 in site A. In Gevokizumab, the critical residues N53 and S52 are within the 4.5 Å of the IL-1 $\beta$  receptor in its crystal structure with IL-1 $\beta$  (PDB ID: 1itb) (Vigers et al., 1997). N53 makes non-bonded contacts with the receptor. D86 in the antibody binding site makes H-bond and non-bonded interactions with IL-1 $\beta$ .

In the case of antibody AAL160-bound IL-1 $\beta$  (bottom right in Figure 7), the key residues showing the highest fluctuations are D54 in the receptor binding site B and I143, which are far from the antibody binding site. In addition to these residues, K27, which is in site A, appears as a key residue. Moreover, L67 in the AAL160 binding site and its neighbor Y68 are also significant. Here, L67 makes non-bonded contact with the heavy chain of the antibody. Also, K27 is a very critical residue that makes H-bond, non-bonded contact, as well as a salt bridge with the IL-1 $\beta$  receptor.

#### 4. Discussion

This computational study investigated the effect of four different antibodies binding to IL-1 $\beta$ . The aim of the study is to reveal critical residues that are affected by antibody binding to IL-1 $\beta$  and determine any allosteric effect of studied antibodies on IL-1 $\beta$ . For this aim, four antibody-bound crystal structures of IL-1 $\beta$  and its apo form were first subjected to the ClustENMD unbiased enhanced sampling method to generate diverse conformers. Then, these conformers were used in two different machine learning methods. PCA was used to analyze the diversity in IL-1 $\beta$  ensembles. PCA results indicate that the total number of generations used in ClustENMD analysis is critical in producing diverse ensembles, and more generations would yield more distinct conformers.

Later, LDA was used to detect differences in apo and antibody-bound IL-1 $\beta$  ensembles. The computational investigation of four different antibodies binding to IL-1 $\beta$  using LDA revealed long-range allosteric effects on the IL-1 $\beta$  cytokine. Three of these antibodies, namely IgG26, Canakinumab, and AAL160, directly interact with the IL-1 $\beta$  from its receptor binding sites A or B. Only Gevokizumab binds IL-1 $\beta$  far from its receptor binding site. Some of the critical residues determined using LDA pinpoint either site A or B, which are the IL-1 $\beta$  receptor interaction sites, or another antibody's binding site, showing long-range allosteric effects of these antibodies. In another crystal structure of IL-1 $\beta$ , a local but large conformational change (near 11 Å) exists on the loop (comprising residues 47-55, PDB ID: 8c3u) (Hommel et al.,

2023). Interestingly, both Gevokizumab and AAL160 binding affect a few residues on this loop (comprising residues 47-55), which is far from their binding site.

On the other hand, LDA results for the IgG26- and Canakinumab-bound IL-1 $\beta$  highlight the region comprising residues 109-112 and 145. The residue K109 makes a salt bridge and non-bonded contacts with the IL-1 $\beta$  receptor accessory protein (PDB ID: 3040) (Wang et al., 2010), and E111 has non-bonded contacts, whereas D145 makes a hydrogen bond. This region is also a binding site in another cytokine, IL-36, which is a member of the IL-1 family and structurally quite similar to IL-1 $\beta$ . A recently discovered antagonist molecule binds IL-36 and is shown to inhibit psoriasis in a 3D human skin model with psoriasis (PDB ID: 6p9e) (Todorović et al., 2019). This region might be a potential binding site for the modulation of human IL-1 $\beta$  and needs further investigation.

The human IL-1β cytokine also plays a role in different types of cancer. When the mutation data on IL-1ß using the cBioPortal web server (Cerami et al., 2012; de Bruijn et al., 2023; Gao et al., 2013), where users can access critical mutations in 10,953 cancer patients, is analyzed, it was revealed that three key residues from LDA, namely N129 (from IgG26-bound) and K65 (from Canakinumabbound), are the missense mutations observed in patients with uterine endometrioid carcinoma whereas Y68 (from AAL160-bound) is a nonsense mutation observed in a lung adenocarcinoma patient. Thus, further investigation of the interactions between the mutant forms of IL-1ß and corresponding antibodies might enlighten the effect of the mutation on their modulatory mechanism and help develop better antibodies for the patients having this specific mutation, serving in personalized medicine.

The experimental studies focused on the combination therapies of two anti-IL-1\beta antibodies, namely Gevokizumab and Canakinumab, showed their better modulatory effectiveness on IL-1ß compared to single antibody treatment (Diwanji et al., 2023). Notably, the LDA results for these antibodies pinpoint distinct affected regions on IL-1\u00e1s. Therefore, this might be one of the reasons why combination therapies of these antibodies are more effective on IL-1\beta, and further analysis is needed on the dynamics of IL-1 $\beta$  in complex with both antibodies. This study reveals novel insights into the antibodymediated modulation of IL-1β. Critical residues, which pinpoint potential binding sites in human IL-1β, are determined using ClustENMD and LDA. The findings of the study underscore the role of computational tools in allosteric networks, unraveling complex mechanistic insights to optimize antigen-targeted biologics.

#### **Author Contributions**

The percentages of the author' contributions are presented below. The author reviewed and approved the final version of the manuscript.

	A.U.
С	100
D	100
S	100
DCP	100
DAI	100
L	100
W	100
CR	100
SR	100
PM	100
FA	100

C=Concept, D= design, S= supervision, DCP= data collection and/or processing, DAI= data analysis and/or interpretation, L= literature search, W= writing, CR= critical review, SR= submission and revision, PM= project management, FA= funding acquisition.

#### **Conflict of Interest**

The author declared that there is no conflict of interest.

#### **Ethical Consideration**

Ethics committee approval was not required for this study because there was no study on animals or humans.

### Acknowledgements

AU acknowledges the financial support from the projects at İzmir Institute of Technology (Project no: AUDP-2022-İYTE-3-0041). Google Colab free computing resources are also used in this study.

#### References

Amadei A, Linssen ABM, Berendsen HJC. 1993. Essential dynamics of proteins. Proteins, 17(4).

Atilgan AR, Durell SR, Jernigan, RL, Demirel MC, Keskin O, Bahar I. 2001. Anisotropy of fluctuation dynamics of proteins with an elastic network model. Biophys J, 80(1): 505–515.

Berman HM, Westbrook J, Feng Z, Gilliland G, Bhat TN, Weissig H, Shindyalov IN, Bourne PE. 2000. The Protein Data Bank. Nucleic Acids Res, 28 (1).

Blech M, Peter D, Fischer P, Bauer MMT, Hafner M, Zeeb M, Nar H. 2013. One Target - Two Different Binding Modes: Structural Insights into Gevokizumab and Canakinumab Interactions to Interleukin-1 $\beta$ . J Mol Biol, 425(1).

Cerami E, Gao J, Dogrusoz U, Gross BE, Sumer SO, Aksoy BA, Jacobsen A, Byrne CJ, Heuer ML, Larsson E, Antipin Y, Reva B, Goldberg AP, Sander C, Schultz N. 2012. The cBio Cancer Genomics Portal: An open platform for exploring multidimensional cancer genomics data. Cancer Discov, 2(5).

de Bruijn I, Kundra R, Mastrogiacomo B, Tran TN, Sikina L, Mazor T, Li X, Ochoa A, Zhao G, Lai B, Abeshouse A, Baiceanu D, Ciftci E, Dogrusoz U, Dufilie A, Erkoc Z, Lara EG, Fu Z, Gross B, Haynes C, Heath A, Higgins D, Jagannathan P, Kalletla K, Kumari P, Lindsay J, Lisman A, Leenknegt B, Lukasse P, Madela D, Madupuri R, van Nierop P, Plantalech O, Quach J, Resnick AC,

Rodenburg SYA, Satravada BA, Schaeffer F, Sheridan R, Singh J, Sirohi R, Sumer SO, van Hagen S, Wang A, Wilson M, Zhang H, Zhu K, Rusk N, Brown S, Lavery JA, Panageas KS, Rudolph JE, LeNoue-Newton ML, Warner JL, Guo X, Hunter-Zinck H, Yu TV, Pilai S, Nichols C, Gardos SM, Philip J, Kehl KL, Riely GJ, Schrag D, Lee J, Fiandalo MV, Sweeney SM, Pugh TJ, Sander C, Cerami E, Gao J, Schultz N. 2023. Analysis and visualization of longitudinal genomic and clinical data from the AACR project GENIE Biopharma Collaborative in cBioPortal. Cancer Res, 83(23).

DeLano WL. 2020. The PyMOL molecular graphics system, version 2.3. In Schrödinger LLC, New York, USA, pp. 14-45.

Dinarello CA. 2014. An expanding role for interleukin-1 blockade from gout to cancer. Molecular Medicine, 20.

Diwanji R, O'Brien NA, Choi JE, Nguyen B, Laszewski T, Grauel AL, Yan Z, Xu X, Wu J, Ruddy DA, Piquet M, Pelletier MR, Savchenko A, Charette LS, Rodrik-Outmezguine V, Baum J, Millholland JM, Wong CC, Martin AM, Dranoff G, Pruteanu-Malinici I, Cremasco V, Sabatos-Peyton C, Jayaraman P. 2023. Targeting the IL1b pathway for cancer immunotherapy remodels the tumor microenvironment and enhances antitumor immune responses. Cancer Immunol Res, 11(6).

Doruker P, Atilgan AR, Bahar, I. 2000. Dynamics of proteins predicted by molecular simulations and analytical approaches: Application to  $\alpha$ -amylase inhibitor. Proteins: Structure, Function and Genetics, 40(3): 512–524.

Eastman P, Pande VS. 2010. OpenMM: A hardware-independent framework for molecular simulations. Comput Sci Eng, 12(4).

Eastman P, Swails J, Chodera JD, McGibbon RT, Zhao Y, Beauchamp KA, Wang LP, Simmonett AC, Harrigan MP, Stern CD, Wiewiora RP, Brooks BR, Pande VS. 2017. OpenMM 7: Rapid development of high performance algorithms for molecular dynamics. PLoS Comput Biol, 13(7).

Fischman S, Levin I, Rondeau JM, Štrajbl M, Lehmann S, Huber T, Nimrod G, Cebe R, Omer D, Kovarik J, Bernstein S, Sasson Y, Demishtein A, Shlamkovich T, Bluvshtein O, Grossman N, Barak-Fuchs R, Zhenin M, Fastman Y, Twito S, Vana T, Zur N, Ofran Y. 2023. Redirecting an anti-IL-1 $\beta$  antibody to bind a new, unrelated and computationally predicted epitope on hIL-17A. Commun Biol, 6(1).

Gao J, Aksoy BA, Dogrusoz U, Dresdner G, Gross B, Sumer SO, Sun Y, Jacobsen A, Sinha R, Larsson E, Cerami E, Sander C, Schultz N. 2013. Integrative analysis of complex cancer genomics and clinical profiles using the cBioPortal. Sci Signal, 6(269).

Guo B, Fu S, Zhang J, Liu B, Li Z. 2016. Targeting inflammasome/IL-1 pathways for cancer immunotherapy. Sci Rep, 6.

Hommel U, Hurth K, Rondeau JM, Vulpetti A, Ostermeier D, Boettcher A, Brady JP, Hediger M, Lehmann S, Koch E, Blechschmidt A, Yamamoto R, Tundo Dottorello V, Haenni-Holzinger S, Kaiser C, Lehr P, Lingel A, Mureddu L, Schleberger C, Blank J, Ramage P, Freuler F, Eder J, Bornancin F. 2023. Discovery of a selective and biologically active low-molecular weight antagonist of human interleukin-1β. Nat Commun, 14(1).

Humphrey W, Dalke A, Schulten K. 1996. VMD: Visual molecular dynamics. J Mol Graph, 14(1).

Kaynak BT, Zhang S, Bahar I, Doruker P. 2021. ClustENMD: efficient sampling of biomolecular conformational space at atomic resolution. Bioinformatics, 37(21).

Kuo WC, Lee CC, Chang YW, Pang W, Chen HS, Hou SC, Lo SY, Yang AS, Wang AHJ. 2021. Structure-based development of human Interleukin-1β-specific antibody That Simultaneously Inhibits Binding to Both IL-1RI and IL-1RAcP. J Mol Biol, 433(4).

Owyang AM, Issafras H, Corbin J, Ahluwalia K, Larsen P, Pongo E, Handa M, Horwitz AH, Roell MK, Haak-Frendscho M, Masat L.

- 2011. XOMA 052, a potent, high-affinity monoclonal antibody for the treatment of IL-1 $\beta$ -mediated diseases. MAbs, 3(1).
- Pedregosa F, Varoquaux G, Gramfort A, Michel V, Thirion B, Grisel O, Blondel M, Prettenhofer P, Weiss R, Dubourg V, Vanderplas J, Passos A, Cournapeau D, Brucher M, Perrot M, Duchesnay É. 2011. Scikit-learn: Machine learning in Python. J Machine Learning Research, 12.
- Ridker PM, Everett BM, Thuren T, MacFadyen JG, Chang WH, Ballantyne C, Fonseca F, Nicolau J, Koenig W, Anker S.D, Kastelein JJP, Cornel JH, Pais P, Pella D, Genest J, Cifkova R, Lorenzatti A, Forster T, Kobalava Z, Vida-Simiti L, Flather M, Shimokawa H, Ogawa H, Dellborg M, Rossi PRF, Troquay RPT, Libby P, Glynn RJ. 2017. Antiinflammatory therapy with canakinumab for atherosclerotic disease. New England J Med, 377(12).
- Ridker PM, MacFadyen JG, Thuren T, Everett B, Libby P, Glynn RJ, Lorenzatti A, Krum H, Varigos J, Siostrzonek P, Sinnaeve P, Fonseca F, Nicolau J, Gotcheva N, Genest J, Yong H, Urina-Triana M, Milicic D, Cifkova R, Vettus, R, Koenig W, Anker S. D, Manolis A. J, Wyss F, Forster T, Sigurdsson A, Pais P, Fucili A, Ogawa H, Shimokawa H, Veze I, Petrauskiene B, Salvador L, Kastelein J, Cornel JH, Klemsdal T. O, Medina F, Budaj A, Vida-Simiti L, Kobalava Z, Otasevic P, Pella D, Lainscak M, Seung K. B, Commerford P, Dellborg M, Donath M, Hwang J. J, Kultursay H, Flather M, Ballantyne C, Bilazarian S, Chang W, East C, Forgosh L, Harris B, Ligueros M, Bohula E, Charmarthi B, Cheng S, Chou S, Danik J, McMahon G, Maron B, Ning M. M, Olenchock B, Pande R, Perlstein T, Pradhan A, Rost N, Singhal A, Taqueti V, Wei N, Burris H, Cioffi A, Dalseg A. M, Ghosh N, Gralow J, Mayer T, Rugo H, Fowler V, Limaye A. P, Cosgrove S, Levine D, Lopes R, Scott J, Hilkert R, Tamesby G, Mickel C, Manning B, Woelcke J, Tan M, Manfreda S, Ponce T, Kam J, Saini R, Banker K, Salko T, Nandy P, Tawfik R, O'Neil G, Manne S, Jirvankar P, Lal S, Nema D, Jose J, Collins R, Bailey K, Blumenthal R, Colhoun H, Gersh B. 2017.

- Effect of interleukin- $1\beta$  inhibition with canakinumab on incident lung cancer in patients with atherosclerosis: exploratory results from a randomised, double-blind, placebocontrolled trial. The Lancet, 390(10105).
- Sakuraba S, Kono H. 2016. Spotting the difference in molecular dynamics simulations of biomolecules. J Chem Physics, 145(7).
  Sims JE, Smith DE. 2010. The IL-1 family: Regulators of immunity.
  In Nature Reviews Immunology, 10 (2).
- Todorović V, Su Z, Putman CB, Kakavas SJ, Salte KM, McDonald HA, Wetter JB, Paulsboe SE, Sun Q, Gerstein CE, Medina L, Sielaff B, Sadhukhan R, Stockmann H, Richardson PL, Qiu W, Argiriadi MA, Henry RF, Herold J. M, Shotwell JB, McGaraughty SP, Honore P, Gopalakrishnan SM, Sun CC, Scott VE. 2019. Small molecule IL-36γ antagonist as a novel therapeutic approach for plaque psoriasis. Sci Rep, 9(1).
- Uyar A, Dickson A. 2021. Perturbation of ACE2 structural ensembles by SARS-CoV-2 spike protein binding. J Chem Theory Comput, 17(9).
- Uyar A, Karamyan VT, Dickson A. 2018. Long-range changes in neurolysin dynamics upon inhibitor binding. J Chem Theory Comput, 14(1).
- Vigers GPA, Anderson LJ, Caffes P, Brandhuber BJ. 1997. Crystal structure of the type-I interleukin-1 receptor complexed with interleukin-1β. Nature, 386(6621).
- Wang D, Zhang S, Li L, Liu X, Mei K, Wang X. 2010. Structural insights into the assembly and activation of IL-1 $\beta$  2 with its receptors. Nat Immunol, 11(10).
- Wong CC, Baum J, Silvestro A, Beste MT, Bharani-Dharan B, Xu S, Wang YA, Wang X, Prescott MF, Krajkovich L, Dugan M, Ridker, PM, Martin AM, Svensson EC. 2020. Inhibition of IL1β by canakinumab may be effective against diverse molecular subtypes of lung cancer: An exploratory analysis of the CANTOS trial AC. Cancer Res, 80(24).